

Estimation of Optimal Slip for Traction Force Improvement of a Mobile Manipulator

A.M.H.S. Abeykoon¹, Kouhei Ohnishi², Fellow, IEEE

¹ A.M.H.S. Abeykoon, Department of System Design Engineering, Keio University, Yokohama, JAPAN
e-mail : harsha@sum.sd.keio.ac.jp

² Kouhei Ohnishi, Department of System Design Engineering, Keio University, Yokohama, JAPAN
e-mail: ohnishi@sd.keio.ac.jp

Abstract— In this paper, a traction control method for a two wheel mobile robot is presented. Traction force acting on a wheel is dependent upon the dynamic frictional coefficient and the reaction force acting on each wheel. It is proposed to obtain the maximum traction force by selecting the best value for slip percentage as well as selecting a suitable value for the reaction force. Reaction force variation is achieved by changing the centre of gravity (COG) of the mobile robot. Two electric motors are used to drive the two wheel manipulator. Optimum slip ratio which maximizes the traction force is calculated dynamically.

I. INTRODUCTION

TODAY the Electric wheeled manipulators are extensively used in outer space experiments, factories and places where humans are not easily accessible. Electric motors are much more controllable than the engine driven vehicles. Motor torque generation is quick and accurate. Further, motors can be fixed to each wheel unlike engines. Advanced control strategies can be easily adopted to electric motor driven vehicles as different parameters like current, voltage, energy etc. can be measured easily.

Mobile manipulators can be literally a subset of electric vehicles. But this should not always be the case. A mobile manipulator can be driven by a non electrical energy source. However in general the differences of mobile manipulators (MM) and Electric Vehicles (EV) can be briefed as follows. There are some basic differences between mobile manipulators and electric vehicles.

Usually EVs are expected to travel longer distances. Driver is expected to command the EV using an accelerating command. EVs are made to achieve high speeds. In contrary MMs are made to travel shorter distances at relatively low speed. MMs are normally used do specific tasks like outer space experiments. MMs can be commanded real-time like in an EV or a path can be commanded to follow. In specific

terms the maximum traction can be attained at a slip which is greater than zero.

If a robotic manipulator is expected to work autonomously it has to identify the environment. There should be sensors to identify obstacles and terrain condition. Road conditions including friction properties of the terrain, provide indispensable contribution for the safe locomotion of the robot. If a wheel slip occurs, the path will be lost. Heavy slip may prevent the robot for further movements. Slip may decrease the traction. Many researches have been done to prevent slip. On the other hand there are relatively low number of researches been done to improve the traction. However in terms of improving the traction, slip is not always undesirable.

There are several advantages of improving the traction force. Slip can be changed or controlled by changing the traction force. Improving the traction force will increase the load that the mobile robot can transport. On the other hand mobile robot can be designed with lesser weight if the traction force can be maximized.

If the mobile manipulator is expected to travel autonomously in a changing terrain, slip can affect the traction force. When a manipulator is moving, sliding and driving forces are acting on it. When the slip of the wheels is high, manipulator tends to slide. Slide force takes its maximum value when the slip is zero. When the slip is increasing, the slide force decreases exponentially. However the effect of sliding is very less since mobile manipulators are not expected to move at a very high speed. Therefore, in this paper, slipping control is only discussed.

Slip ratio λ is defined as follows where V_w is the wheel speed and V is the vehicle ground speed.

$$\lambda = (V_w - V) / V_w \quad (1)$$

Fig.1 shows the typical shape of the Friction coefficient - slip ratio ($\mu-\lambda$) curve for two different terrains.

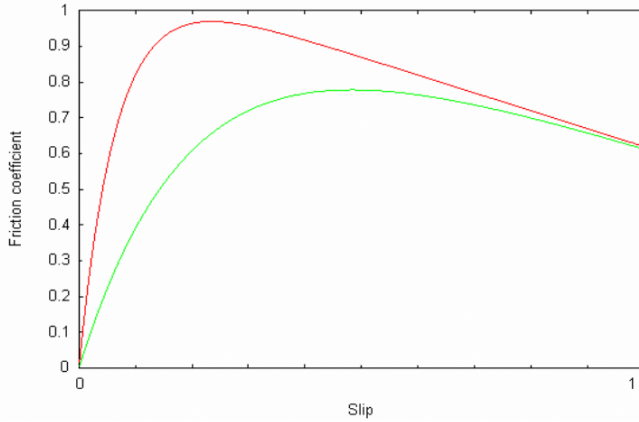


Fig. 1. ($\mu-\lambda$) curves

As for the above figure, it can be noted that when the slip ratio increases dynamic frictional coefficient μ also increases. Then it starts decreasing from the maximum point. If there is a method to operate at this maximum μ , mobile manipulators can achieve the maximum traction force provided that there is no change in the wheel reaction force. The point at which the reaction force is maximum is called as the optimum slip ratio.

Friction force exchanged by the wheel and the road is given by the equation (2).

$$F = N \mu(\text{Slip}) \quad (2)$$

Where F is the traction force and N is the normal force (reaction force) acting on the wheel. $\mu(\text{Slip})$ is the friction coefficient corresponding to the slip as of the $\mu - \lambda$ curve. As for equation (2), traction force is a function of N and $\mu(\text{Slip})$. When N is a constant, F can be maximized by selecting the optimum $\mu(\text{Slip})$. When N is a variable, both optimum $\mu(\text{Slip})$ and N maximizes the traction force.

Y. Hori and others have implemented traction control strategy based on regulation of desired slip ratio decided by the road condition estimator [2],[3]. Unfortunately these strategies are designed for high speed vehicles like cars. One primary objective of our study was to compute the optimal slip ratio. Novel method to estimate the optimal slip ratio is proposed. This method can be used for any unknown terrain. Previous researches have used terrain data for the optimal slip estimation. Further this method is simple and the computation requires less resources.

Road condition estimation algorithm is similar to the estimator proposed by [2]. However it is customized for two wheeled low speed mobile robot. As for the equation (2) traction force can be increased by changing reaction force. Reaction force is changed by changing the centre of gravity (COG) of the mobile manipulator. As for this proposed method, when a wheel is slipping COG is moved towards the slipping wheel such that the traction force is increased.

II. CONSTRUCTION

A. Physical Construction

For this research two wheeled mobile manipulator is used. Both wheels are driven separately by two DC motors. Both motors can be controlled independently. Ground speed is measured using a non-driven wheel. Wheel speed is measured using two rotary encoders which are attached to the wheels. Changing the gravity location is achieved through the manipulation of an arm, which is already attached to the mobile robot.

B. Kinematics

Kinematics model, which is used, is shown in Fig .2

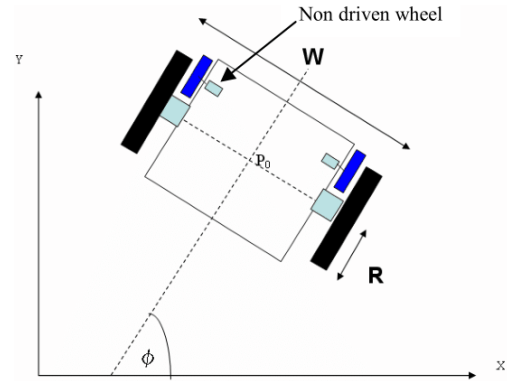


Fig. 2. Kinematics model -world coordinate

Where,

W : Thread of the robot

R : Radius of driving wheel

ϕ : Attitude angle

Angle of rotation of right and left wheels can be represented as equation (3).

$$\theta = [\theta_r, \theta_l]^T \quad (3)$$

Position and attitude angle can be represented as (4).

$$X = [x, y, \phi]^T \quad (4)$$

Then the direct kinematics equation can be represented as (5)

$$\begin{bmatrix} \dot{x}_0 \\ \dot{y}_0 \\ \dot{\phi}_0 \end{bmatrix} = \begin{bmatrix} \frac{R\cos\phi}{2} & \frac{R\cos\phi}{2} \\ \frac{R\sin\phi}{2} & \frac{R\sin\phi}{2} \\ \frac{2}{R} & \frac{2}{R} \\ \frac{1}{W} & \frac{1}{W} \end{bmatrix} \begin{bmatrix} \dot{\theta}_r \\ \dot{\theta}_l \end{bmatrix} \quad (5)$$

where Jacobian matrix J is represented as (6).

$$J = \begin{bmatrix} \frac{R\cos\phi}{2} & \frac{R\cos\phi}{2} \\ \frac{R\sin\phi}{2} & \frac{R\sin\phi}{2} \\ \frac{2}{R} & \frac{2}{R} \\ \frac{1}{W} & \frac{1}{W} \end{bmatrix} \quad (6)$$

In order to calculate inverse kinematic equations, (5) is differentiated and (8) can be obtained where

$$Jaco^+ = \frac{1}{R} \begin{bmatrix} \cos\phi & \sin\phi & \frac{W}{2} \\ \cos\phi & \sin\phi & -\frac{W}{2} \end{bmatrix} \quad (7)$$

$$\ddot{\theta} = J_{aco}^+(\phi) \cdot \dot{\dot{X}} + \dot{J}_{aco}^+(\phi) \cdot \dot{X} \quad (8)$$

By neglecting the inverse Jacobean derivative, (9) can be obtained.

$$\ddot{\theta} = J_{aco}^+(\phi) \cdot \dot{\dot{X}} \quad (9)$$

C Dynamics

Dynamics of the mobile robot can be described as follows. Torques of right and left wheels can be calculated as follows.

$$\begin{bmatrix} \tau_r \\ \tau_l \end{bmatrix} = M_\theta \cdot \begin{bmatrix} \ddot{\theta}_r \\ \ddot{\theta}_l \end{bmatrix} \quad (10)$$

Here,

$$M_\theta = \begin{bmatrix} \frac{M}{4} + \frac{J}{W^2} + \frac{J_w}{R^2} & \frac{M}{4} - \frac{J}{W^2} \\ \frac{M}{4} - \frac{J}{W^2} & \frac{M}{4} + \frac{J}{W^2} + \frac{J_w}{R^2} \end{bmatrix} \quad (11)$$

M : Mass of the mobile robot

J : Inertia of mobile robot around axis vertical to x-y plane

J_w : Inertia of each wheel

D Dead-Reckoning

In order to estimate position and attitude dead-reckoning is used. Estimated values of x and y positions are found as follows.

$$x_k = x_{k-1} + v \cdot \cos\left(\frac{\phi_k + \phi_{k-1}}{2}\right) \cdot \Delta t \quad (12)$$

$$y_k = y_{k-1} + v \cdot \sin\left(\frac{\phi_k + \phi_{k-1}}{2}\right) \cdot \Delta t \quad (13)$$

Here,

Subscript k indicates their values at time k and subscript k-1 indicates their values at time k-1.

v : Velocity of the robot in world coordinate at time k
 Δt : Sampling time

Attitude angle is calculated as follows.

$$\phi = \frac{R}{W} \cdot (\theta_r - \theta_l) \quad (14)$$

III. CONTROL SYSTEM

Block diagram of the control system is shown in the Fig. 3.

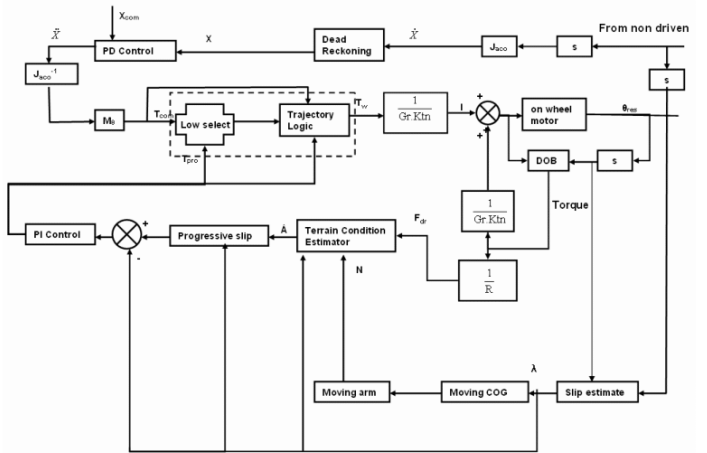


Fig. 3. Control Block diagram

A. Low Select and Trajectory Logic

As for Fig. 3, low select and trajectory logic function is marked with a dotted box. Box is fed with two values. They are T_{pro} and T_{com}. T_{com} is coming from the users input containing desired path information. T_{pro} is calculated from the road condition estimator. It is the optimal torque based on the slip data.

If low select function selects T_{pro} value of left or right wheel, that implies that wheel is slipping. In other words user is

commanding a value which is over than the maximum possible torque value. If at least one value of T_{pro} out of both wheels is selected, selected torque does not contain user's path information.

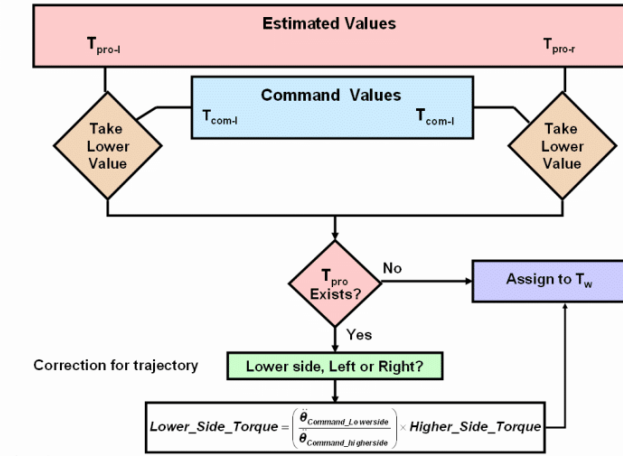


Fig. 4. Low select and trajectory logic

Trajectory logic function is there to preserve the path information successfully whilst selecting lower value for torque to satisfy slip data. Trajectory logic function together with low select function is depicted as Fig. 3.

B. On wheel motor and Disturbance observer

Each on wheel motor incorporates a disturbance observer. This serves two purposes. First one is to compensate the modeling errors and external disturbances. Second purpose is to estimate the disturbance torque which is proportional to the driving force acting on the wheel. When the disturbance torque is divided by the wheel radius, driving force can be estimated.

C. Slip Estimate

Slip ratio can be easily calculated from the non driven wheel input and the on wheel motor output.

D. Moving COG

Slip rations can be directly used to move the COG. If the left wheel slips or if the left wheel slip is more than the right wheel, moving arm is commanded to move towards left wheel to increase the reaction force acting on that wheel. This will decrease the reaction force acting on the right wheel. Moving arm settles in a position where there is less difference between the slips.

E. Moving arm

Reaction force variation is modeled using the following simple manipulator model. Forces on two wheels are N_l and

N_r . Width of the manipulator is "a". Weight of the vehicle except the moving arm is considered as "mg". Weight of the moving arm is considered as "Mg". Mg is acting "x" distance away as shown in the diagram.

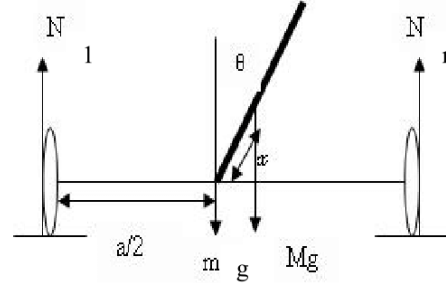


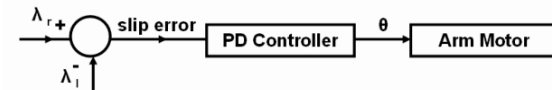
Fig. 5. Normal force variation

As the θ varies, N_l and N_r values will be changed according to the following equations.

$$N_l + N_r = (m+M)g \quad (15)$$

$$a/2 \cdot mg + (a/2 + x \sin \theta) Mg = a N_r \quad (16)$$

Fig. 6 depicts the arm controller. Left and right wheel slips are used to calculate the slip error. It calculates the arm angle using a PD controller.



Slip Error	Meaning	Action
Positive	Right slipping	Move arm towards the right wheel
Negative	Left slipping	Move arm towards the left wheel

Fig. 6. Arm Controller

F. Terrain condition estimator

If the moving arm position is known, the reaction force acting on each wheel can be calculated as shown before. Driving force can be calculated from the disturbance observer.

Dynamic frictional coefficient can be calculated as follows.

$$\mu(\text{Slip}) = \frac{\text{Driving force on the wheel}}{\text{Reaction force on wheel}} \quad (17)$$

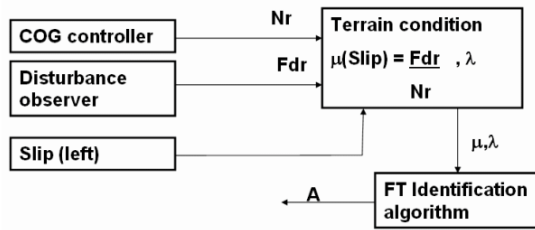


Fig. 7. Terrain Condition estimation

Gradient of μ - λ curve A is defined as follows.

$$A = \frac{d\mu}{d\lambda} \quad (18)$$

To eliminate the effect of sudden changes a well known adaptive identification method, fixed trace (FT) algorithm is used.

G. Progressive slip

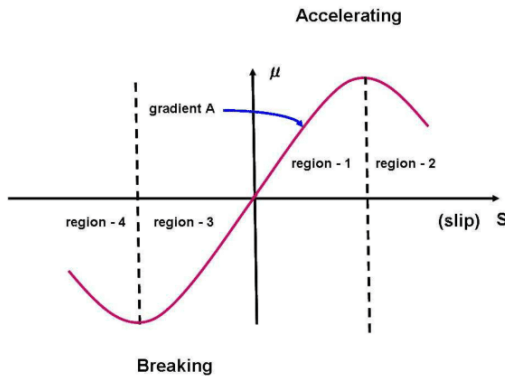


Fig. 8. Slip in regions

As for Fig.8. gradient A is positive until the slip reaches the optimal value. A will be negative when the robot is operating on the undesirable region. Therefore progressive slip is a simple optimal slip estimation process. When A is positive it indicates that the current level of optimal slip is more than the present slip. On the other hand when A is negative, optimal slip should be below the present level of slip. μ - S curve can be divided in to four regions according to the A gradient and S slip. In precise terms, when the A is very high that indicates the optimum slip is closer. On the other hand when the present slip is high, the optimal slip should also be closer. To incorporate these characteristics, author has used a simple estimation method of optimal slip. It is presented as (19).

$$\text{optimal slip} = \text{present slip} \times (1 + x + y) \quad (19)$$

The value x is dependent on the gradient A and value y is dependent on the current slip. Table 1 shows the way the estimation is being done by varying x and y . As for Figure 5.13, μ - λ curve can be divided in to four regions according to the slip's sign and the sign of A .

Table 1: Slip in regions

Region 1 and 3			Region 2 and 4		
$A > 0$ Optimum = Current slip * (1+X+Y)			$A < 0$ Optimum = Current slip * (1+X+Y)		
$0 < A < 0.5$	$0.5 < A < 10000$	$10000 < A$	$-0.5 < A < 0$	$-10000 < A < -05$	$-10000 < A$
$X=0, Y=0$	$X=2A/10000, Y=S/2$	$X=0, Y=S/2$	$X=0, Y=0$	$X=2A/10000, Y=-S/2$	$X=0, Y=-S/2$

IV. EXPERIMENT RESULTS

Mobile manipulator used is made for Indoor use only. It has a work span of 6m. The slip is artificially exerted to the system by using a slippery material. A vinyl tape is pasted on the floor where the manipulator is expected to run. Left wheel was run through this heavy slippery material.

Fig 9. shows the time response of the slip. Slip is at its maximum when the manipulator starts moving as it accelerates. Then is run through the slippery material between 4s to 5s. There is a clear increase of slip as the left wheel runs through the slippery material.

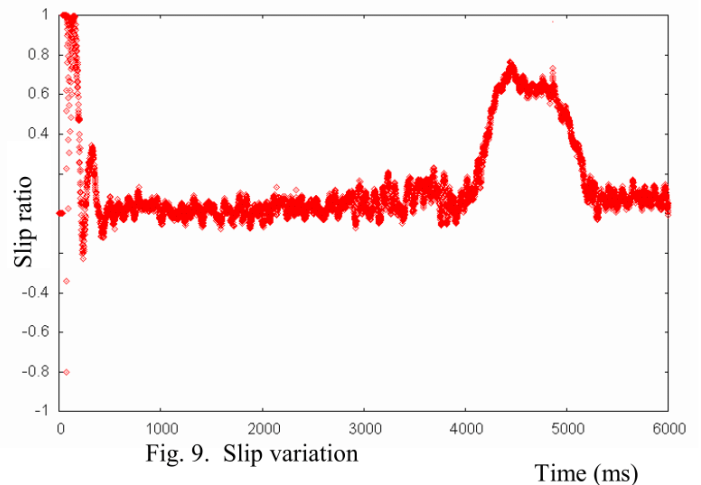


Fig. 9. Slip variation

Fig. 10 shows the position response of the manipulator in the above slip condition. Mobile manipulator is commanded to move towards x direction. Despite of the slip, trajectory is not much distorted due to the slip regulating function. However the position response is not exactly fits to the x axis. This is because, the system does not eliminate the

slip fully instead it operates at a value which is optimal for the traction.

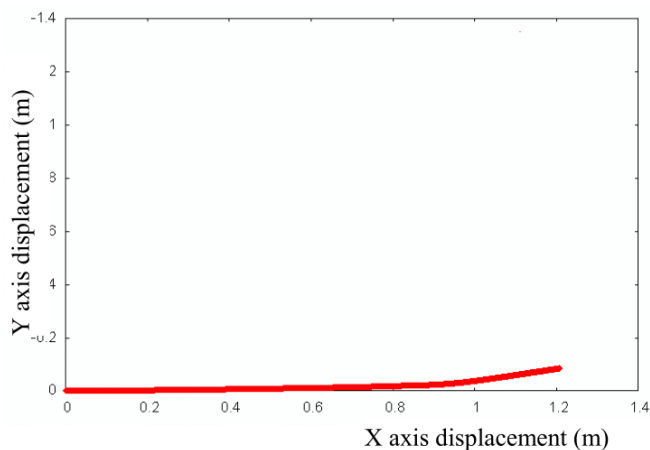


Fig. 10. : Position response

Fig. 11 depicts the optimal slip ratio estimated by the system as for the above slip. When there is little slip in the system, it estimates high optimal slip as more and more slip is possible. This region is shown as tractive region in the figure. During the high slipping, system suddenly estimates lower slip which will increase the adhesion.

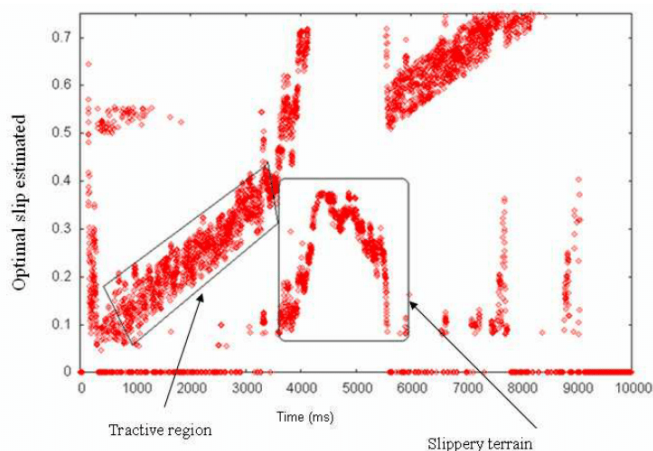


Fig. 11. Optimal slip ratio estimated

V. CONCLUSION

This method does not directly calculate the target dynamic frictional coefficient. Instead the method used here is an iterative estimation method. Novel idea of changing COG is proposed to improve the traction force and to increase the adhesion. Road condition estimator has been customized for two wheel manipulators where the speed concerned is relatively low as in the case of mobile manipulator. Non driven wheel is used to measure the ground speed of the

mobile manipulator. However this method assumes the non driven wheels does not slip when the driven wheel slips. This is a simple demonstration method, which is different from the practical reality. Non driven wheel itself slips in heavy slip conditions. However optical methods are there to calculate the vehicle ground speed fairly accurately. Therefore such an accurate method has to be used for future studies for better results. Driving force itself can be used as a measure of slip as it is proposed in this text. Further research is possible in this area.

Change of the COG, might affect lateral forces acting on the manipulator. Therefore there should be a strike of balance between the traction improvement by the COG change and its adverse effects to the mobile manipulator. Further studies are possible in this area as well. In this approach, the optimal speed of the mobile manipulator was set by using the optimal slip. Used mobile manipulator was intended to be used for indoor experiments. Robot has a work space of only 6m, which is relatively shorter for detailed analysis of slipping and estimation of road conditions. Instead of using artificial slip, real terrains should be used for better analysis.

ACKNOWLEDGMENT

Author would like to convey his sincere gratitude to Keio University, Japanese Government and the people of Japan for the financial support given.

REFERENCES

- [1] D.Caltabiano, D.Ciancitto, G.Muscato, "Experimental Results on a Traction Control Algorithm for Mobile Robots in Volcano Environment", in *Proc. of IEEE Transactions on Robotics and Automation* Vol.5, 26 April-1 May 2004, pp.4375-4380
- [2] K. Furukawa, Y. Hori, "Recent Development of Road Condition Estimation Techniques for Electric Vehicle and their Experimental Evaluation using the Test EV- UOT March I and II", in *Proc. of IEEE Transactions on Industrial Electronics*, Vol.2, 2003, pp. 925 - 930.
- [3] Y. Hori, Y. Toyoda and Y. Tsuruoka, "Traction control of electric vehicle based on the estimation of road surface condition-basic experimental results using the test EV "UOT Electric March", in *Proc. of IEEE transactions on Power Conversion*, Vol.1, August 1997
- [4] J.V.D. Burg and P. Blazevic, "Anti-Lock Braking and Traction Control Concept for All-Terrain Robotic Vehicles", in *Proc. of the IEEE International Conference on Robotics and Automation Albuquerque, New Mexico* Vol.2, April 1997, pp. 1400 - 1405
- [5] K.Ohnishi, M.Shibata, T.Murakami, "Motion Control for Advanced Mechatronics", in *Proc. of IEEE Transactions on Mechatronics*, Vol.1, No.1, March 1996, pp.56-67.
- [6] H. Abeykoon and K. Ohnishi, "Traction Force Improvement of a Mobile Manipulator", in the *Papers of Technical Meeting on Industrial Instrumentation and Control, IEEE Japan*, 2005 March, pp.121-125
- [7] M.Kondo, K.Ohnishi, "Constructing a Platform of Robust Position Estimation for Mobile Robot by ODR", in *Proc. of IEEE Transactions on Advanced Motion Control* March 2004, pp.263-268